

# Electronic Normal Modes and Polarization Waves in Translational Polymer Helices. Application to Fully Extended Poly[(R)-β-aminobutyric acid] Chains

Jon Applequist

Department of Biochemistry, Biophysics, and Molecular Biology, Iowa State University, Ames, Iowa 50011

Received: March 6, 2000; In Final Form: May 12, 2000

The electronic normal modes of a finite translational polymer helix are found to be well approximated by sinusoidal standing waves of electronic polarization with either even or odd symmetry with respect to inversion through the chain center. The dipole and rotational strengths of the normal modes are expressed as products of two types of sums over the wave: (i) lattice sums which are independent of the structure within the unit cell and (ii) cell sums which contain the structural information of the unit cell. Owing primarily to the behavior of the lattice sums at low wavenumber  $k$  of the polarization wave, the dipole and rotational strengths of a single low- $k$  mode tend to dominate the absorption and circular dichroic spectra. The dispersion relation between frequency and wavenumber is derived for the polarization waves, giving further relations for the phase velocity and group velocity of a traveling polarization wave. The results are illustrated by calculations for fully extended poly[(R)-β-aminobutyric acid] chains.

## Introduction

A translational helix is a structure generated by translating a unit cell repeatedly in one dimension, with no accompanying rotation. The term “one-dimensional crystal” would be appropriate, though in the case of a polymer chain capable of taking on such a structure, it is more useful to classify it among the various possible helical conformations of the polymer. (In this context we regard the unit cell as containing one residue, as any helix with an exact repeat in  $N$  residues could be regarded as a translational helix if the unit cell were defined as one repeat.)

The poly(β-amino acids) in fully extended form constitute translational helices. This structure has been found in intermolecularly hydrogen-bonded form in fibers and films of long-chain, chiral poly(β-aminobutyric acid) [(βAbu) $_N$ ].<sup>1,2</sup> Small β-peptides have also been found in similar or related sheet forms in crystals and in solution.<sup>3–5</sup> In the preceding paper in this issue<sup>6</sup> Bode and I have shown that our model for electronic absorption and circular dichroism (CD) of single extended chains, such as might occur in solution under appropriate conditions, predicts unusual features which appear to be related to the unique character of the translational helix. In particular, the model produces an absorption spectrum which is dominated by a single electronic normal mode, giving a single Lorentzian peak. Likewise, the CD spectrum tends to be dominated by the same mode, giving a single peak that is coincident in wavelength and shape with that of the absorption spectrum. The CD spectrum is also unusual in that the system of amide  $\pi$ - $\pi^*$  chromophores is planar in a translational helix, so that the rotational strength of the  $\pi$ - $\pi^*$  band comes entirely from interaction of the chromophores with the chiral environment of nonchromophoric atoms.

The purpose of this paper is to examine the normal modes predicted by our model for a translational helix to discover how the unusual spectral features are related to the structure. It is found that the normal modes are well approximated by sinusoidal standing waves of electronic polarization and that all of the spectral properties can be understood by the behavior of such waves. The known polymer (βAbu) $_N$ , which derives its

chirality from a methyl side chain on C $^{\beta}$  (here taken as the  $R$  configuration), is taken as an example to illustrate the predicted wave properties.

## The Model

Our model for a translational helix consists of an array of  $N$  unit cells, each generated from a neighboring unit cell by translation through a distance  $a$  along a specified axis. The unit cell contains  $P$  polarizable point particles representing atoms or groups of atoms. On each such point lie a number of linear electronic oscillators, giving a total of  $S$  oscillators in the unit cell. The properties of the system are to be calculated from the coordinates and dipole polarizabilities of all oscillators in the array, assuming that the particles interact only by way of the electric fields of their induced electric dipole moments. The position of oscillator  $j$  relative to the origin of the unit cell is  $\mathbf{r}_j$  ( $j = 1, \dots, S$ ). The orientation of oscillator  $j$  is given by unit vector  $\hat{\mathbf{u}}_j$ .

For simplicity we consider the case in which the unit cell contains only one dispersive oscillator, which is designated by index  $j = 1$  and is located at the unit cell origin ( $\mathbf{r}_1 = 0$ ). The polarizability  $\alpha_1$  of the dispersive oscillator is assigned a Lorentzian frequency dependence given by

$$\alpha_1 = \frac{d_0 \hat{\mathbf{u}}_1 \hat{\mathbf{u}}_1}{\omega_0^2 - \omega^2 + i\gamma\omega} \quad (1)$$

where  $d_0$  and  $\omega_0$  are the dipole strength ( $\text{cm}^3 \text{s}^{-2}$ ) and angular frequency of resonance, respectively, of the isolated oscillator,  $\omega$  is the frequency of the light, and  $\gamma$  is the damping coefficient. [Here we replace wavenumber  $\bar{\nu}$  used in previous papers<sup>7</sup> with  $\omega = 2\pi c\bar{\nu}$ , where  $c$  is the velocity of light. Hence, the dipole strength  $D_0$  of the previous papers is replaced by  $d_0 = 4\pi^2 c^2 D_0$ .] All other oscillators are taken to be nondispersive with constant polarizabilities of the form

$$\alpha_j = \alpha_j \hat{\mathbf{u}}_j \hat{\mathbf{u}}_j \quad (2)$$

Thus, nonchromophoric atoms are represented by three mutually perpendicular oscillators with equal polarizabilities. The NC'O group is represented by the dispersive oscillator of eq 1 plus three unequal, mutually perpendicular nondispersive oscillators representing polarizability contributions from electronic transitions well above the frequency range of the chromophore.

### Polarization Waves

The basic equation of the dipole interaction model is<sup>8</sup>

$$\mathbf{A}\boldsymbol{\mu} = \mathbf{E} \quad (3)$$

where  $\mathbf{A}$  is the interaction matrix,  $\boldsymbol{\mu}$  is the column matrix of dipole moments of all oscillators, and  $\mathbf{E}$  is the column matrix of external electric fields at each oscillator. All matrix elements are expressed in DeVoe form.<sup>9</sup> In particular,  $\mathbf{A}$  has diagonal elements  $\alpha_j^{-1}$  and off-diagonal elements  $\hat{\mathbf{u}}_j \cdot \mathbf{T}_{jl} \cdot \hat{\mathbf{u}}_l$ , where  $\mathbf{T}_{jl}$  is the dipole field tensor.

We wish to determine the possible electronic polarization motions of the system in the absence of an external field. The problem is greatly simplified by partitioning of the matrices into blocks for subsystem 1, containing the dispersive oscillators, and subsystem 2, containing the nondispersive oscillators. The partitioned form of eq 3 for this problem is

$$\begin{pmatrix} \mathbf{A}_{11}(\omega) & \mathbf{A}_{12} \\ \mathbf{A}_{21} & \mathbf{A}_{22} \end{pmatrix} \begin{pmatrix} \boldsymbol{\mu}_1 \\ \boldsymbol{\mu}_2 \end{pmatrix} = \begin{pmatrix} \mathbf{0} \\ \mathbf{0} \end{pmatrix} \quad (4)$$

where subscripts 1 and 2 on each block represent the subsystems whose oscillators are referred to in the rows or columns, respectively, of that block, and where it is recognized that the 11 block contains all of the frequency dependence of  $\mathbf{A}$ . The consequences of this partitioning have been developed in detail previously<sup>10</sup> for the determination of normal modes. For the present purposes we note that eq 4 leads to the relations for the dipole moments

$$\mathbf{A}_{11}'(\omega)\boldsymbol{\mu}_1 = 0 \quad (5)$$

$$\boldsymbol{\mu}_2 = -\mathbf{A}_{22}^{-1}\mathbf{A}_{21}\boldsymbol{\mu}_1 \quad (6)$$

where

$$\mathbf{A}_{11}'(\omega) = \mathbf{A}_{11}(\omega) - \mathbf{A}_{12}\mathbf{A}_{22}^{-1}\mathbf{A}_{21} \quad (7)$$

Using eq 1 with neglect of the damping term, we have

$$\mathbf{A}_{11}'(\omega) = \mathbf{A}_{11}'(0) - (\omega^2/d_0)\mathbf{I} \quad (8)$$

where  $\mathbf{I}$  is the identity matrix. From eqs 5 and 8 we have

$$\mathbf{A}_{11}'(0)\boldsymbol{\mu}_1 = (\omega^2/d_0)\boldsymbol{\mu}_1 \quad (9)$$

which corresponds to the classical equation of motion for a system of undamped, coupled oscillators having a time dependence of the form  $e^{i\omega t}$ . Let  $\mu_{mj}$  be the component of  $\boldsymbol{\mu}$  for oscillator  $j$  in unit cell  $m$ . For an infinitely long translational helix the equation of motion for the chromophores is satisfied by traveling waves of the form<sup>11</sup>

$$\mu_{m1} = \frac{1}{2}c_1 e^{i(\omega t + mka + \delta)} \quad (10)$$

where  $c_1$  is a constant,  $k$  is the wave vector, related to the wavelength  $\lambda$  by  $k = \pm 2\pi/\lambda$ , and  $\delta$  is an arbitrary phase angle. This wave is called here a "polarization wave". In what follows

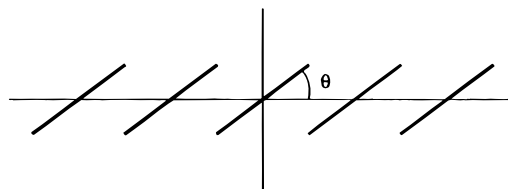


Figure 1. Array of chromophore axes in a translational helix.

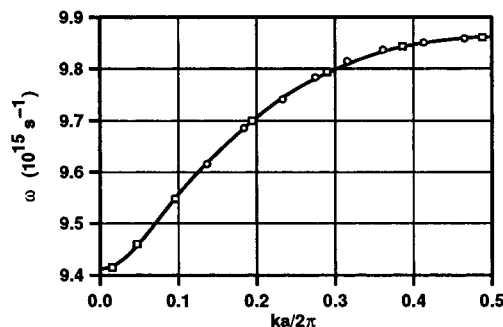


Figure 2. Dispersion relation for  $(\beta\text{Abu})_N$ : (—) calculated by eq 12 for  $N = 15$ ; (○) normal modes for  $N = 10$ ; (□) normal modes for  $N = 30$ .

it will be shown that such a wave is a good approximation for fairly short translational helices as well as long ones.

### Dispersion Relation

The equation of motion determines the dispersion relation, which relates  $\omega$  and  $k$ . We insert eq 10 into eq 9 and obtain

$$\omega^2 e^{i(\omega t + pka + \delta)} = d_0 \sum_{m=1}^N [\mathbf{A}_{11}'(0)]_{pm} e^{i(\omega t + mka + \delta)} \quad (11)$$

for  $p = 1, \dots, N$ . On rearranging and taking the real part, we have

$$\omega^2 = d_0 \sum_{m=1}^N [\mathbf{A}_{11}'(0)]_{pm} \cos[(m-p)ka] \quad (12)$$

This relation would be independent of  $p$  for an infinitely long chain. But the diagonal elements of  $\mathbf{A}_{11}'(0)$  are relatively constant for chromophores more than 2–3 cells from the ends of the chain, and the off-diagonal elements diminish rapidly with the distance between chromophores. Hence, eq 12 is nearly independent of  $p$  for values well removed from the ends of a finite chain. We will apply the relation using  $p = [(N+1)/2]$ , where the brackets denote the integer part. The following are important consequences of eq 12: (i)  $\omega(-k) = \omega(k)$ ; (ii)  $\omega(k) = \omega(k + 2\pi/a)$ ; (iii)  $\omega(k)$  may be either an increasing or a decreasing function of  $k$  in the range  $0 \leq k \leq \pi/a$ , depending on whether the  $\mathbf{A}_{11}'(0)$  elements for near neighbors are negative or positive, respectively. If the system consisted only of the array of oscillators in Figure 1, these elements would be positive for  $\theta > 54.7^\circ$  and negative for  $\theta < 54.7^\circ$ .

Figure 2 shows the dispersion relation calculated for  $(\beta\text{Abu})_{15}$  from eq 12. For this and all other results reported here for  $(\beta\text{Abu})_N$ , the structure was generated as described in the preceding paper in this issue,<sup>6</sup> and the calculations included the interactions among all atoms and amide  $\pi-\pi^*$  chromophores in the system. The abscissa is  $ka/2\pi = a/\lambda$ . The unit cell length  $a$  is 4.824 Å.<sup>6</sup> The chromophore parameters (which are equivalent to those of data set  $H_y$ )<sup>12</sup> are  $d_0 = 1.133 \times 10^8 \text{ cm}^3 \text{ s}^{-2}$ ,  $\omega_0 = 10.85 \times 10^{15} \text{ s}^{-1}$ , and  $\hat{\mathbf{u}}_1$  oriented at  $9.3^\circ$  with respect

to the N–C' bond toward the O atom. The collective behavior of the unit cell contents is like that of an oscillator oriented at angle  $\theta = 13.9^\circ$ ,<sup>6</sup> corresponding to the region of negative interaction noted above.

The dispersion curves calculated for  $N \geq 7$  are all in good agreement with the curve in Figure 2, with only slight variations for the shorter chains. As noted above, the same values of  $\omega$  are obtained when the sign of  $k$  is reversed, and the curve oscillates with period 1 on the abscissa scale. The range  $-0.5 \leq ka/2\pi \leq +0.5$  is known as the first Brillouin zone.<sup>13</sup> Values of  $k$  outside this range have no physical significance, as they correspond to wavelengths shorter than  $2a$ .

### Electronic Normal Modes

The normal modes of the system are solutions to eq 4 corresponding to standing waves. In the partially dispersive normal mode method, the problem is reduced to the solution of eq 9 in the form of the eigenvalue problem:<sup>10</sup>

$$\mathbf{A}_{11}'(0)\mathbf{t}_1^{(n)} = (\omega_n^2/d_0)\mathbf{t}_1^{(n)} \quad (13)$$

where  $\omega_n^2$  is the  $n$ th eigenvalue corresponding to eigenvector  $\mathbf{t}_1^{(n)}$ , whose components are dipole moments of the chromophores obeying the orthonormality condition

$$\mathbf{t}_1^{(n)\text{T}}\mathbf{t}_1^{(n')} = \delta_{nn'}d_0/4\pi^2c^2 \quad (14)$$

where superscript T denotes transpose and  $\delta_{nn'}$  is the Kronecker delta. The factor  $4\pi^2c^2$  preserves the units of  $\mathbf{t}_1^{(n)}$  used in our previous papers. There are  $N$  normal modes in accordance with the  $N$  degrees of freedom in the system of chromophores.

In the following sections we approximate a normal mode by a superposition of two waves of the form of eq 10 with opposite signs of  $k$ , giving the standing wave

$$\mu_{m1}^{(n)} = c_1 e^{i\omega_n t} \cos(mk_n a + \delta) \quad (15)$$

where the index  $n$  specifies a particular normal mode, usually in order of increasing  $\omega_n$ . Then the components of  $\mathbf{t}_1^{(n)}$ , denoted  $\tau_{m1}^{(n)}$  ( $m = 1, \dots, N$ ), are

$$\tau_{m1}^{(n)} = c_1(mk_n a + \delta) \quad (16)$$

The normalization constant  $c_1$  depends on  $\delta$ , as shown in the following section.

It should be noted that the discrete set of  $\omega_n$  values are the only pure frequencies of free oscillation consistent with the equations of motion for a given chain length. Equation 12 expresses  $\omega$  and  $k$  as continuous variables, though only for infinite chains do all points on the dispersion curve represent possible waves in the absence of an external force.

### Symmetry of Normal Modes

A principle from the theory of molecular vibrations applies to the electronic normal modes as well: every normal mode must belong to an irreducible representation (symmetry species) of the molecule at rest.<sup>14</sup> Thus, the symmetries of the normal modes are governed by the symmetry of the molecule. The normal mode method<sup>10</sup> requires no information on the symmetry of the molecule, though the eigenvectors describing the normal modes automatically belong to whatever symmetry species are required by the structure.

Our translational helix does not necessarily have any symmetry elements. However, it turns out that the normal modes

**TABLE 1: Number of Normal Modes of Each Symmetry Species in a Translational Helix of  $N$  Unit Cells**

N	$A_g$	$B_u$
even	$N/2$	$N/2$
odd	$(N-1)/2$	$(N+1)/2$

whose frequencies are correlated with the resonant frequency of the chromophore have very nearly the symmetry governed by the symmetry of the array of chromophores, without regard to the presence of nonchromophoric oscillators.

Consider, then, a system consisting solely of the array of  $N$  chromophore oscillator axes spaced at uniform intervals along a translational axis and oriented at angle  $\theta$  with respect to the translational axis, as shown in Figure 1 for  $N = 5$ . The system belongs to point group  $C_{2h}$ , though higher symmetries occur if  $\theta = 0$  or  $\pi/2$ . From the method of characters of symmetry operations<sup>14</sup> one finds that all normal modes must be of symmetry species  $A_g$  or  $B_u$ , the number of modes of each species being those shown in Table 1. There are no degenerate modes. For our purposes it is sufficient to specify the symmetries of the modes by their behavior with respect to inversion through the inversion center, indicated by the subscripts g (symmetric with respect to inversion) and u (antisymmetric with respect to inversion).

Assuming that the normal modes are given by eq 16, the following phases satisfy the symmetry requirements:

$$\delta = \begin{cases} -(N+1)k_n a/2 & (\text{u-modes}) \\ -(N+1)k_n a/2 + \pi/2 & (\text{g-modes}) \end{cases} \quad (17)$$

A shift in  $\delta$  from these values by  $\pm\pi$  also satisfies the corresponding symmetry, as it simply reverses the signs of the dipole moments.

By normalization of  $\mathbf{t}_1^{(n)}$  according to eq 14, one finds

$$c_1 = \frac{d_0^{1/2}}{2\pi c} \left( \frac{N}{2} \mp \frac{\sin Nk_n a}{2 \sin k_n a} \right)^{-1/2} \quad (18)$$

where the upper sign applies to g-modes and the lower sign to u-modes.

### Tests of Normal Mode Wave Forms

Figure 3 shows the normal mode components of the amide chromophores in  $(\beta\text{Abu})_{10}$ . The bars show  $\tau_{m1}^{(n)}$  for each chromophore  $m1$  in each normal mode  $n$  calculated directly by eqs 13 and 14, which assume no particular wave form. It is seen that every odd-numbered mode has u symmetry and every even-numbered mode has g symmetry. These symmetries are not exact, as expected from the fact that the full system does not have  $C_{2h}$  symmetry; however, the discrepancies between "symmetric" components are 1% or less, and are not apparent in the figure.

The curves in Figure 3 were calculated by eqs 16–18, using  $k_n$  values obtained from  $\omega_n$  by interpolation in eq 12. The values are given in Table 2. The curves agree well with the components indicated by the bars, showing that the simple sinusoidal wave form is an accurate representation of the normal modes. Note that this conclusion is not evident from the bars alone.

The dispersion relation of Figure 2 provides a further test. The figure shows a number of data points for the eigenfrequencies  $\omega_n$  calculated for  $(\beta\text{Abu})_N$  with  $N = 10$  and 30, and using  $k$  values estimated from a spline fit (a crude sine curve) to eigenvector components such as those shown by the bars in Figure 3. These data confirm that (i) eq 12 is consistent with

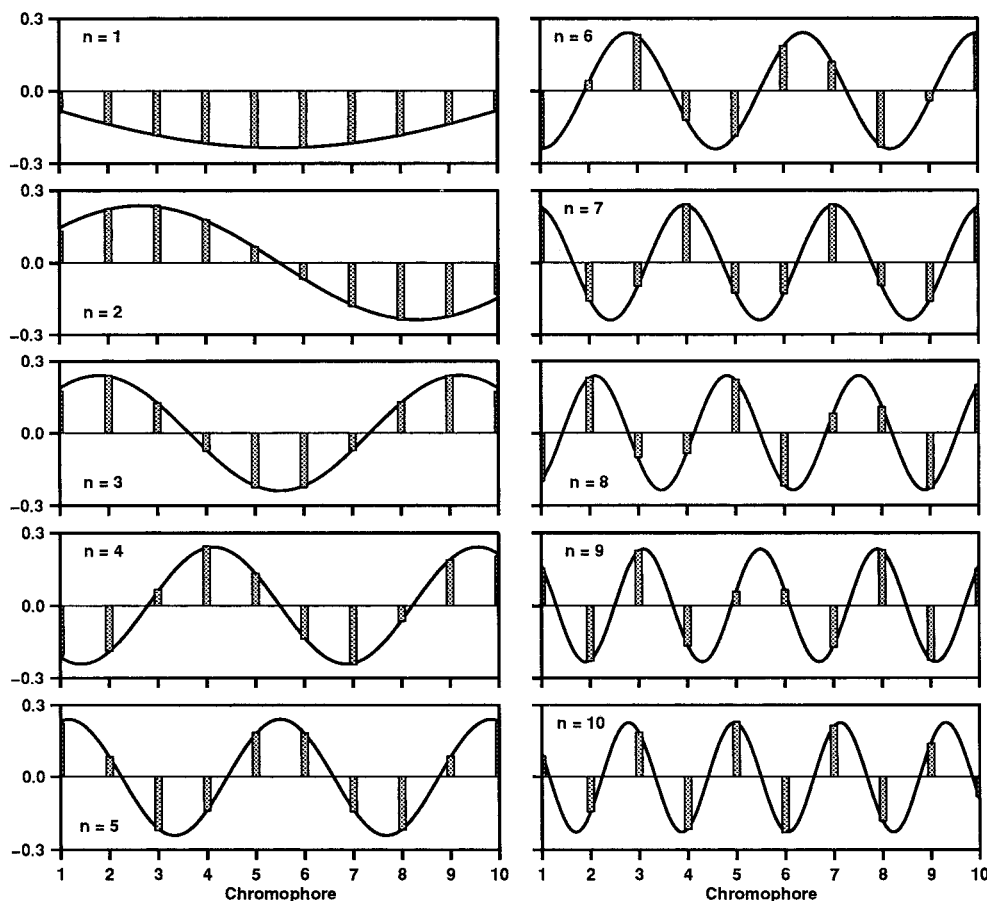


**Figure 3.** Normal modes of fully extended  $(\beta\text{Abu})_{10}$ . The ordinate is  $\tau_{m1}^{(n)}$  in units of  $10^{-7} \text{ cm}^{1/2}$ . Bars show eigenvector components on amide chromophores. Curves show wave forms calculated by eq 16. Modes are numbered in order of increasing frequency.

**TABLE 2: Frequencies and Wave Vectors of Normal Modes of Fully Extended  $(\beta\text{Abu})_{10}$**

$n$	$\omega_n (10^{15} \text{ s}^{-1})$	$k_n a / 2\pi$	$n$	$\omega_n (10^{15} \text{ s}^{-1})$	$k_n a / 2\pi$
1	9.4503	0.0432	6	9.7836	0.2787
2	9.5336	0.0878	7	9.8146	0.3259
3	9.6159	0.1351	8	9.8365	0.3695
4	9.6859	0.1841	9	9.8507	0.4169
5	9.7413	0.2302	10	9.8585	0.4600

an accurate normal mode analysis and (ii) the same dispersion relation is valid for a wide range of chain lengths.

A further noteworthy feature of the normal modes is that they do not obey, even approximately, a periodic boundary condition, which requires that the component on particle  $N + 1$  be identical to the component on particle 1. This condition has been applied to related problems on one-dimensional systems as a simplified means of obtaining normal modes.<sup>15,16</sup>

### Dipole Moments of Nondispersive Oscillators

The eigenvector block  $\mathbf{t}_2^{(n)}$  contains the components  $\tau_{pj}^{(n)}$  of the normal mode dipole moments of the nondispersive oscillators, with  $p = 1, \dots, N$  and  $j = 2, \dots, S$ . Let

$$\tau_{pj}^{(n)} = c_j e^{i(pk_n a + \delta + \theta_j)} \quad (19)$$

where  $c_j$  and  $\theta_j$  are amplitudes and phase angles determined by eq 6; i.e.

$$c_j e^{i(pk_n a + \delta + \theta_j)} = -c_1 \sum_{m=1}^N (\mathbf{A}_{22}^{-1} \mathbf{A}_{21})_{pj,m1} e^{i(mk_n a + \delta)} \quad (20)$$

Here eq 16 has been incorporated in complex form, recognizing that the real parts of both  $\tau_{pj}^{(n)}$  and  $\tau_{m1}^{(n)}$  are the actual eigenvector components. Equation 20 is rearranged to give

$$c_j e^{i\theta_j} = -c_1 \sum_{m=1}^N (\mathbf{A}_{22}^{-1} \mathbf{A}_{21})_{pj,m1} e^{i(m-p)k_n a} \quad (21)$$

Thus,  $c_j$  and  $\theta_j$  are determined from the absolute value and polar angle of the expression on the right. Note that  $\theta_1 = 0$  by eq 16. Equation 21 is nearly independent of  $p$  for values more than 2–3 unit cells from the ends. In the following we take  $p = [(N + 1)/2]$ .

### Dipole Strength and Rotational Strength

An electric dipole moment  $\boldsymbol{\mu}^{(n)}$  and magnetic dipole moment  $\mathbf{m}^{(n)}$  of the  $n$ th normal mode are defined by<sup>10</sup>

$$\boldsymbol{\mu}^{(n)} = \sum_{m=1}^N \sum_{j=1}^S \tau_{mj}^{(n)} \hat{\mathbf{u}}_j \quad (22)$$

$$\mathbf{m}^{(n)} = \sum_{m=1}^N \sum_{j=1}^S \tau_{mj}^{(n)} (\mathbf{R}_m + \mathbf{r}_j) \times \hat{\mathbf{u}}_j \quad (23)$$

where  $\mathbf{R}_m$  is the origin of unit cell  $m$  with respect to a molecular coordinate origin. We take  $\mathbf{R}_m = ma\hat{\mathbf{e}}$ , where  $\hat{\mathbf{e}}$  is a unit vector along the translation axis of the helix. The normal mode dipole strength  $D_n$  and rotational strength  $R_n$  are<sup>17</sup>



$$D_n = (Re)\boldsymbol{\mu}^{(n)} \cdot (Re)\boldsymbol{\mu}^{(n)} \quad (24)$$

$$R_n = (Re)\boldsymbol{\mu}^{(n)} \cdot (Re)\mathbf{m}^{(n)} \quad (25)$$

When the wave form of eq 19 is introduced,  $D_n$  and  $R_n$  become functions of a continuous variable  $k$ , which will be denoted  $D(N,k)$  and  $R(N,k)$ . By combining eqs 19 and 22–25, one obtains

$$D(N,k) = [L_1(N,k)]^2 C_1(N,k) \quad (26)$$

$$R(N,k) = [L_1(N,k)]^2 C_2(N,k) + L_1(N,k) L_2(N,k) C_3(N,k) \quad (27)$$

where the lattice sums  $L_1$  and  $L_2$  are

$$L_1(N,k) = \frac{\sin(Nka/2)}{\sin(ka/2)} \quad (28)$$

$$L_2(N,k) = \frac{(N+1) \sin[(N-1)ka/2] - (N-1) \sin[(N+1)ka/2]}{2(1 - \cos ka)} \quad (29)$$

and the cell sums  $C_1$ ,  $C_2$ , and  $C_3$  are

$$C_1(N,k) = \sum_{j=1}^S \sum_{l=1}^S \left( \frac{\sin \theta_j \sin \theta_l}{\cos \theta_j \cos \theta_l} \right) c_j c_l \hat{\mathbf{u}}_j \cdot \hat{\mathbf{u}}_l \quad (30)$$

$$C_2(N,k) = \sum_{j=1}^S \sum_{l=1}^S \left( \frac{\sin \theta_j \sin \theta_l}{\cos \theta_j \cos \theta_l} \right) c_j c_l \hat{\mathbf{u}}_j \cdot \mathbf{r}_l \times \hat{\mathbf{u}}_l \quad (31)$$

$$C_3(N,k) = \sum_{j=1}^S \sum_{l=1}^S \left( \frac{\sin \theta_j \cos \theta_l}{-\cos \theta_j \sin \theta_l} \right) a c_j c_l \hat{\mathbf{u}}_j \cdot \hat{\mathbf{e}} \times \hat{\mathbf{u}}_l \quad (32)$$

The upper line in the parentheses in eqs 30–32 applies to g-modes and the lower line to u-modes. The  $L_i(N,k)$  come from the sums over unit cells  $m$  in eqs 22 and 23 and are independent of the structure within the unit cell. The  $C_i(N,k)$  come from the sums over oscillators  $j$  in one unit cell; their dependence on  $N$  comes primarily from the normalization of coefficients in eq 18. Notice that the rotational strength comes entirely from the chirality of the unit cell and not that of the lattice for a translational helix.

Figure 4 shows the lattice sums for various  $N$ . Figure 5 shows the cell sums for  $(\beta\text{Abu})_{15}$ . Figure 6 shows  $D(N,k)$  along with the normal mode dipole strengths for various  $(\beta\text{Abu})_N$ . Figure 7 shows  $R(N,k)$  along with the normal mode rotational strengths. It is seen that the region of low  $k$  is dominant for both strength functions, and this is increasingly so as  $N$  increases. This is largely due to the behavior of the lattice sums. The most important finding is that both  $D(N,k)$  and  $R(N,k)$  are largest for the normal mode of lowest  $k$ , in agreement with the normal mode calculations. Likewise, the functions reproduce the strengths of most of the weak modes quite well. These results account for the unusual behavior of calculated absorption and circular dichroic spectra of fully extended poly( $\beta$ -amino acid) chains.<sup>6</sup>

### Wave Velocities

This study has focused mainly on polarization waves as standing waves. The approach produces realistic results in terms of spectra calculated by more accurate methods, and it is therefore relevant to ask whether traveling polarization waves in similar systems have any physical significance. The most important properties of traveling waves are their phase velocities

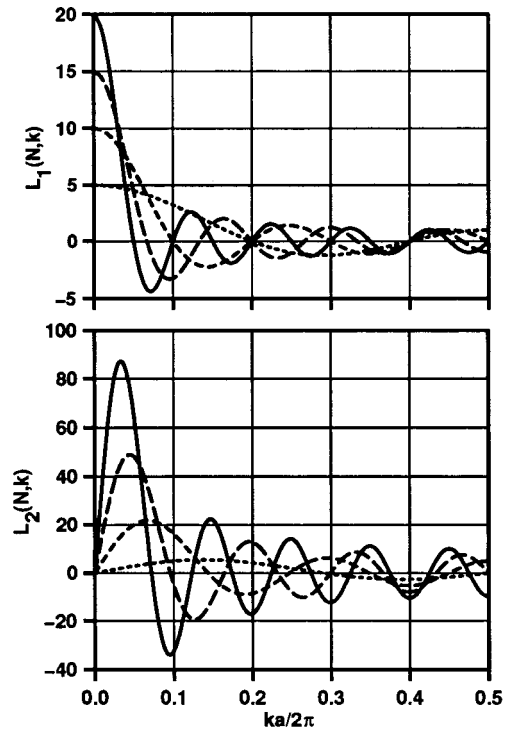


Figure 4. Lattice sums for 1-dimensional lattice with  $N$  unit cells: (---)  $N = 5$ ; (- · - ·)  $N = 10$ ; (—)  $N = 15$ ; (—)  $N = 20$ .

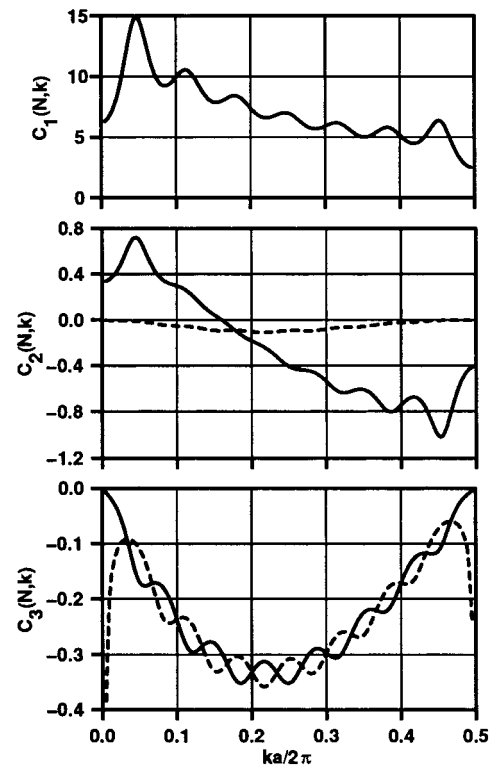
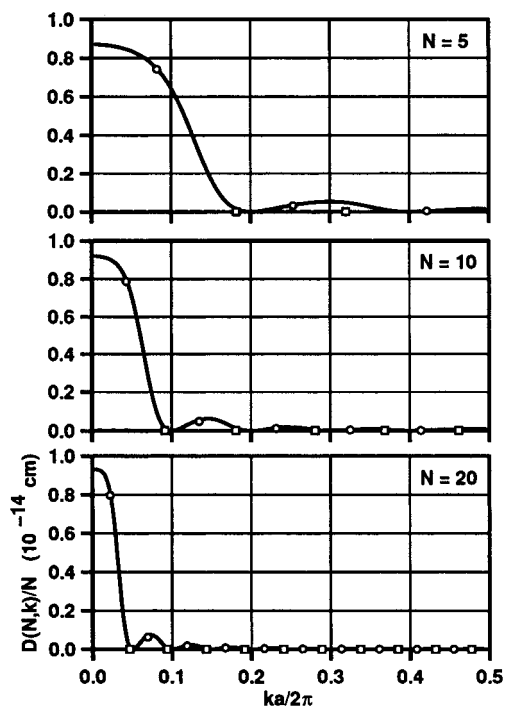


Figure 5. Cell sums for  $(\beta\text{Abu})_{15}$ . The ordinate units are  $10^{-16}$  cm for  $C_1$  and  $10^{-24}$  cm<sup>2</sup> for  $C_2$  and  $C_3$ : (—) u-modes; (---) g-modes. The value of  $C_1$  for g-modes is essentially zero on the scale shown.

$V_p$  and group velocities  $V_g$ . These velocities are of no immediate concern in our study of optical properties, but they help to complete the picture of polarization waves. The velocities are fixed by the relation between  $\omega$  and  $k$  according to<sup>18</sup>

$$V_p = \omega/k \quad (33)$$

$$V_g = d\omega/dk \quad (34)$$



**Figure 6.** Dipole strength function for  $(\beta\text{Abu})_N$ : (—) u-modes. The function for g-modes is essentially zero on the scale shown. Data points show calculations by normal mode analysis: (O) u-modes; (□) g-modes.

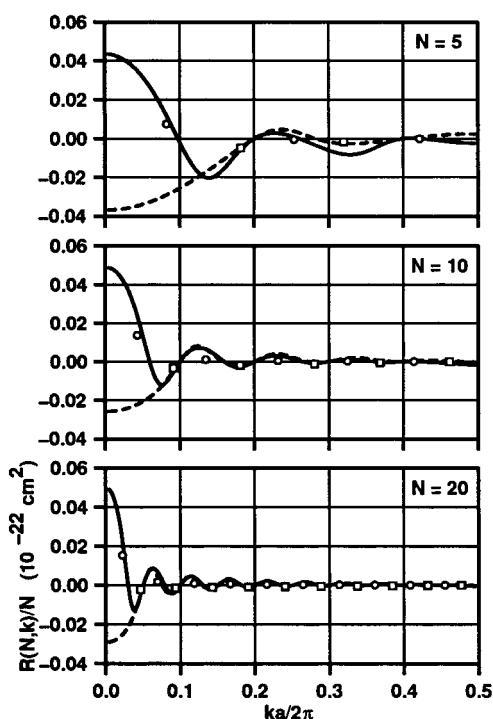


**Figure 7.** Rotational strength function for  $(\beta\text{Abu})_N$ : (—) u-modes; (---) g-modes. Data points show calculations by normal mode analysis: (O) u-modes; (□) g-modes.

The velocities are shown in Figure 8, as calculated for  $(\beta\text{Abu})_{25}$  from eq 12 and its derivative.  $V_p$  is less than the velocity of light over most of the range, though  $V_p \rightarrow \infty$  as  $k \rightarrow 0$ . There is no contradiction to the theory of relativity in this result, according to the resolution of related problems of phase velocities by Sommerfeld.<sup>19</sup>  $V_g$  is closely analogous to the group velocity of excitation waves ("excitons") in the quantum mechanical theory of excitations in crystals.<sup>20</sup> In that case  $V_g$  represents the velocity of migration of excitation in the crystal,

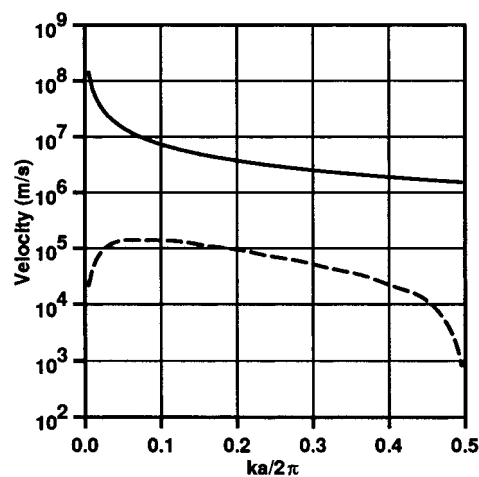


**Figure 8.** Phase and group velocities of polarization waves in  $(\beta\text{Abu})_{25}$ : (—) phase velocity; (---) group velocity.

as expressed by a wave whose amplitude is the coefficient expressing the probability of excitation at each chromophore.<sup>20</sup> The correspondence between exciton theory and the classical polarizability model has been demonstrated for a 3-dimensional crystal by Ball and McLachlan.<sup>21</sup>

## Discussion

The main conclusions of this study are the following.

(1) The electronic normal modes of a finite translational helix are well approximated by sinusoidal standing polarization waves. This conclusion is based on the facts that (i) such wave forms agree accurately with computed eigenvector components, (ii) the relation between frequency and wave vector for such waves agrees with an accurate normal mode analysis, and (iii) the waveforms lead to dipole strengths and rotational strengths of normal modes in agreement with accurate calculations.

(2) The assumption of sinusoidal wave forms leads to expressions for dipole and rotational strengths in terms of products of lattice sums and cell sums; the former are independent of unit cell structure, and the latter contain all the information on the contents of the unit cell. This provides a convenient means of tracing the origins of effects that are otherwise buried in the equations of the eigenvalue equations for the normal modes. The new expressions may also offer computational convenience in some problems, though the eigenvalue equations are more accurate and usually present no computational limitations.

(3) The absorption and circular dichroic spectra of the finite translational helices of  $(\beta\text{Abu})_N$  are dominated by the single normal mode of lowest  $k$ , which has u symmetry. A major reason for this is the large value of the lattice sums  $L_1(N,k)$  and  $L_2(N,k)$  in the low- $k$  region; thus, there should be a tendency for similar spectral behavior in any chiral translational helix. Similar calculations for  $(\beta\text{Amb})_N$  and  $(\beta\text{Chc})_N$ <sup>6</sup> do show the dominance of the low- $k$  mode in both absorption and CD. However, the distribution of rotational strengths among normal modes is rather different in  $(\beta\text{Aib})_N$ ,<sup>6</sup> showing that the cell sums, which are characteristic of the particular unit cell structure, also play an important role in determining the major features of the spectra.

(4) The occurrence of the lowest  $k$  wave at the lowest frequency of the band of normal modes in fully extended poly- $(\beta$ -amino acid) chains arises from the negative interaction matrix elements in eq 12. When these elements are positive, as when  $\theta > 54.7^\circ$  (Figure 1), the lowest  $k$  occurs at the highest frequency.

(5) The normal mode polarization waves do not obey a periodic boundary condition, and the normal modes behave rather differently from those derived from a periodic boundary condition. As Moffitt<sup>16</sup> pointed out in his exciton treatment of general helices, this boundary condition results in exact vanishing of dipole strengths of all normal modes but one for a translational helix of any finite chain length. It can be shown further that the remaining “allowed” normal mode has  $k = 0$  for all chain lengths. These features are contrary to the present results for finite translational helices.

## References and Notes

- (1) Bestian, H. *Angew. Chem., Int. Ed. Engl.* **1968**, *7*, 278.
- (2) Schmidt, E. *Angew. Makromol. Chem.* **1970**, *14*, 185.
- (3) Seebach, D.; Overhand, M.; Kühnle, F. N. M.; Martinoni, B.; Oberer, L.; Hommel, U.; Widmer, H. *Helv. Chim. Acta* **1996**, *79*, 913.
- (4) Krauthäuser, S.; Christianson, L. A.; Powell, D. R.; Gellman, S. H. *J. Am. Chem. Soc.* **1997**, *119*, 11719.
- (5) Seebach, D.; Abele, S.; Gademann, K.; Jaun, B. *Angew. Chem., Int. Ed.* **1999**, *38*, 1595.
- (6) Applequist, J.; Bode, K. A. *J. Phys. Chem. A* **2000**, *104*, 7129.
- (7) Applequist, J. *J. Chem. Phys.* **1979**, *71*, 4332; erratum, *J. Chem. Phys.* **1980**, *73*, 3521.
- (8) Applequist, J.; Carl, J. R.; Fung, K.-K. *J. Am. Chem. Soc.* **1972**, *94*, 2952.
- (9) DeVoe, H. *J. Chem. Phys.* **1965**, *43*, 3199.
- (10) Applequist, J.; Sundberg, K. R.; Olson, M. L.; Weiss, L. C. *J. Chem. Phys.* **1979**, *70*, 1240; erratum, *J. Chem. Phys.* **1979**, *71*, 2330.
- (11) Brillouin, L. *Wave Propagation in Periodic Structures*, 1st ed.; McGraw-Hill: New York, 1946; pp 26–30.
- (12) Bode, K. A.; Applequist, J. *J. Phys. Chem.* **1996**, *100*, 17825; erratum, *J. Phys. Chem. A* **1997**, *101*, 9560.
- (13) Brown, F. C. *The Physics of Solids*; W. A. Benjamin: New York, 1967; p 154.
- (14) Wilson, Jr., E. B.; Decius, J. C.; Cross, P. C. *Molecular Vibrations*; McGraw-Hill: New York, 1955; pp 92–99.
- (15) Born, M.; Huang, K. *Dynamical Theory of Crystal Lattices*; Oxford University Press: London, 1954; pp 55–61.
- (16) Moffitt, W. *J. Chem. Phys.* **1956**, *25*, 467.
- (17) Applequist, J. *J. Chem. Phys.* **1979**, *71*, 1983.
- (18) Born, M. *Atomic Physics*, 5th ed.; Hafner: New York, 1951; pp 330–331.
- (19) Sommerfeld, A. *Optics*; Academic Press: New York, 1964; p 114.
- (20) Davydov, A. S. *Theory of Molecular Excitons*; McGraw-Hill: New York, 1962; pp 35–37, 81.
- (21) Ball, M. A.; McLachlan, A. D. *Proc. R. Soc. London Ser. A* **1964**, *282*, 433.